

The structural performance of axially loaded CFST columns under various loading conditions

Fuyun Huang, Xinmeng Yu* and Baochun Chen

School of Civil Engineering, Fuzhou University, China

(Received June 11, 2011, Revised August 09, 2012, Accepted August 17, 2012)

Abstract. Concrete filled steel tube (CFST) structures have been used widely in high-rise buildings and bridges due to the efficiency of structurally favourable interaction between the steel tube and the concrete core. In the current design codes only one loading condition in the column members is considered, *i.e.*, the load is applied on the steel tube and concrete core at the same time. However, in engineering practice the tube structures may be subjected to various loading conditions such as loading on the concrete core only, preloading on the steel tube skeleton before filling of concrete core, and so on. In this research, a series of comparative experiments were carried out to study the structural performance of concrete filled circular steel tube columns subject to four concentric loading schemes. Then, a generalized prediction method is developed to evaluate the ultimate load capacity of CFST columns subject to various loading conditions. It is shown that the predictions by the proposed method agree well with test results.

Keywords: concrete filled steel tube column; confinement effect; comparative study; loading scheme; generalized method; nominal poisson's ratio; ultimate load capacity

1. Introduction

Concrete filled steel tube (CFST) columns have been used widely in high-rise buildings, underground infrastructures and bridges in recent years. It is predictable that more and more CFST structures will be constructed and become city landmarks or scenic spots.

The commonly used cross sections of CFST can be circular or rectangular (mainly square). Polygonal sections and elliptical sections (Dai *et al.* 2010) are occasionally used. And sometimes, the concrete core is further strengthened by reinforcements (Xiamuxi *et al.* 2012). The advantage of circular CFST columns is the favourable interaction between the steel tube and the concrete core which helps to achieve higher load capacity than simple superposition of the load capacities of the steel tube and concrete core alone. The confinement provided by the steel tube increases the concrete strength. Meanwhile, the existence of concrete core prevents or delays local buckling of the steel tube. The steel is located farthest to the centroid of the CFST members so that maximum moment of inertia can be achieved. Compared with reinforced concrete (RC) bridges, CFST arch bridges weight less and are more ductile, and therefore have better seismic resistance. Compared with steel arch bridges, CFST bridges are much more cost effective. The building can be ascended more quickly compared to reinforced

* Corresponding author, Ph.D., E-mail: xinmengyu@gmail.com

concrete structure since the steelwork, which acts as a permanent framework for concreting, can precede the concrete by several stories (Gourley *et al.* 2008). Furthermore, various erection and closure technologies have been developed to accelerate the construction of CFST arch bridges. These merits enable the booming development of arch bridges. A study by Chen *et al.* (2009) showed that more than 200 CFST arch bridges had been built in China since 1990.

The study of CFST members and their implementation in engineering structures can be dated back to 1950s. The influence of diameter to thickness ratio (D/t) was studied by O'Shea *et al.* (2000) and Gupta *et al.* (2007). Manojkumar *et al.* (2010) used DOE (Design of Experiment) approach to investigate the effect of changes in diameter of the steel tube, wall thickness of the tube, strength of in-fill concrete and length of the column on the axial ultimate load capacity of circular CFST columns. Bahrami *et al.* (2011) used finite element method to study the ultimate axial load capacity and ductility of the columns with various tube wall thicknesses and different cross section shapes and number of stiffeners. Zhu *et al.* (2012) studied numerically the failure mechanism of steel tube columns filled with concrete strengths changing from 30 MPa to 110 MPa. Various simplified ultimate load capacity (UL) prediction methods have been proposed in design methods based on various considerations, such as the EC4 (2004), ACI (1999), AS (1998), LRFD (AISC 2005), JSCE (2006), CECS (1992), DL/T (1999), JCJ (1989), *etc.*. They are all derived from a large number of test data and therefore can achieve reasonable predictions. However, only the situation of loading on the entire section is considered in these methods. It is required to take appropriate measures to prevent slippage between the concrete and steel to ensure the mechanism of composite action (JSCE 2006).

A preliminary consideration is that the steel tube and concrete core form ideally composite action to bear load simultaneously, as the loading type A (abbreviated as LT-A, and hereafter) shown in Fig. 1. Indeed, this is the loading condition most intensively studied and well documented in design codes. According to the functions of the CFST members, load conditions may be quite different in construction. When a CFST column is used as a bridge pier, the load is usually acting on the concrete only (LT-B in Fig. 1). The steel tube is usually used only for the lateral confinement of concrete to improve the strength and ductility of the concrete column. The local buckling of steel tube is not a problem therefore thinner wall tube can be used. The same scheme is also widely used to enhance the seismic resistance of reinforced concrete columns. On the contrary, there is a situation that the concrete core shrinks (or occasionally due to field operation defects) after casting to form a gap at the end of the CFST column so that the load is adversely acting on the steel tube only (LT-C in Fig. 1). When CFST columns are used in high-rise buildings, a general construction procedure is to pump concrete into hollow steel tubes after several storeys above them have been constructed (Liew *et al.* 2009). Therefore the steel tubes are subjected to preloading arising from self-weight and construction imposed loads (LT-D in Fig. 1). Similarly, when CFST members are used as ribs of arch bridges, the ribs are usually set up to sustain the skeleton load before filling of concrete. Composite action can not be formed without hardened concrete inside. The scale of preloading is usually measured by a ratio parameter, β , defined as

$$\beta = \sigma_0 / f_y \quad (1)$$

where σ_0 is the initial axial stress in the steel tube, f_y is the yield stress of steel.

In order to understand the structural behaviour of CFST members subject to various loading conditions, a large number of experiments have been conducted. These tests include CFST members with different loading conditions, cross section shapes, slenderness ratios, short-term or long-term loadings, and so on. A number of tests (Cai 1989, O'Shea 1997, Johansson 2002, Wang 2005) on short

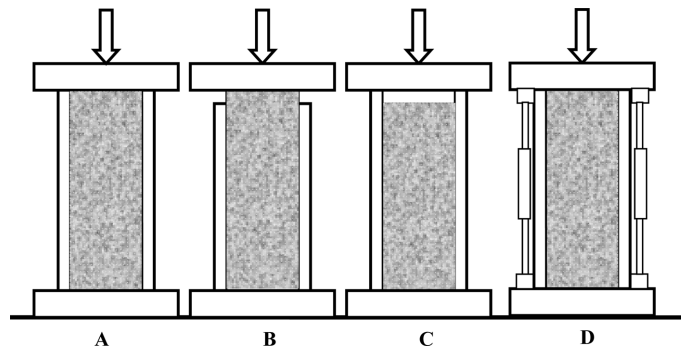


Fig. 1 Loading schemes commonly used in experimental studies

circular-type CFST columns have been done with LT-A, -B or -C loading. It was reported that LT-B could bear the highest load capacity; applying loads on the steel tube only had no evident influence on the load capacity. Johansson *et al.* (2000) tested eleven eccentrically loaded 2500 mm long circular CFST columns. The loads were applied on the concrete core, steel tube or the entire section. It was observed that the load bearing capacity of the column was drastically reduced when the load was applied on the steel section only, and the yielding of the steel tube determined the maximum load. However, this is not necessary true in other loading conditions. In an effort (Starossek *et al.* 2009) to study the interaction between the steel tube and concrete core in CFST columns by natural bond and mechanical shear connectors, seventy one 750 mm or 1200 mm long specimens were tested by applying loads as shown in Fig. 1. It was found that, when the load was applied on the concrete core alone, the maximum longitudinal stress of steel at the ultimate load state was approximately 60% of the yield strength.

Liew and Xiong (2009) tested eleven preloaded or non-preloaded circular CFST columns in three lengths, *i.e.*, 708 mm, 1728 mm and 3078 mm. The cross section diameter was 219 mm; the wall thickness was 6.3 mm. It was observed that the stub columns failed due to squashing whereas the intermediate and long columns failed mainly due to overall buckling. Local buckling of steel tubes was observed in some specimens, but it appeared only in the post-UL range. The study concluded that when the slenderness or preloading ratio was low, the influence of preloading could be ignored. However, the load capacity could be reduced by over 20% when the preloading ratio was high. It was further inferred that preloading might have a more profound effect on the compressive resistance of more slender CFST members due to local buckling of the steel tube. A simplified UL calculation formulation was then proposed by adjusting the strength reduction factor, χ_{pre} , defined in the EC4 (2004), by preloading ratio (refer to Section 3.3 for more details).

The above mentioned researches studied only some types of the loading schemes, such as LT-A-B or LT-A-C or LT-A-D or LT-A-B-C, and lack of peer-to-peer, *i.e.*, the same dimensions and materials and comparison of the ULs under various loading conditions.

This research aims at understanding the CFST column behaviours under various loading conditions: (a) Carrying out a series of experimental studies on the above mentioned four concentric loading schemes, including empty steel tube tests (LT-E); (b) A comparative study on the ULs of CFST columns under various loading conditions; (c) Development of a generalized UL prediction method for CFST columns under various loading conditions.

2. Experimental studies

2.1 Specimen specifications

In order to investigate the influence of different loading conditions on the ultimate strength of CFST columns, a total of 15 CFST specimens and 3 empty steel tubes were fabricated and tested. The steel tubes were welded from Grade Q345 (GB 50017, 2003) steel plates. The outer diameter of the tubes was 108 mm; the tube wall thickness was 4 mm. They were carefully cut and machined to three lengths of short (324 mm), intermediate (1296 mm) and long (1944 mm), so that the two ends were parallel to each other and normal to the longitudinal axis. The relative slenderness, λ , of the short, intermediate and long specimens were 0.13, 0.54 and 0.81, respectively. Because preloading is a normal but not well studied phenomenon in construction, two scales of preloading (LT-D1 ($\beta = 0.25$) and LT-D2 ($\beta = 0.54$)) were studied here. So there were 6 specimens subject to various loading schemes in each length group, namely, LT-A, -B, -C, -D1, -D2 and -E.

The material properties listed in Table 1 were measured before testing. The specimens are abbreviated as "XY", where X denotes the length ($L = \text{long}$, $M = \text{intermediate}$ or $S = \text{short}$) and Y denotes the loading scheme (A, B, C, D1, D2 or E). The geometry of the specimens and the abbreviations used are given in Fig. 2 and Table 2. Apparently, the yield load of empty tube (LT-E loading) is about 440 kN. The preloading ratios can be obtained correspondingly.

Table 1 Material properties of CFST specimens

	Steel Tube	Concrete Core (C50)
Young's Modulus, E_a (MPa)	200000	/
Yield Strength, f_y (MPa)	336.0	/
Ultimate Strength, f_u (MPa)	550.4	/
Poisson's ratio, ν_a	0.286	/
Compressive Strength, f_{cube} (MPa)*	/	54.9 (28-day)

*The cylinder compressive strength is assumed to be $0.8 f_{cube}$.

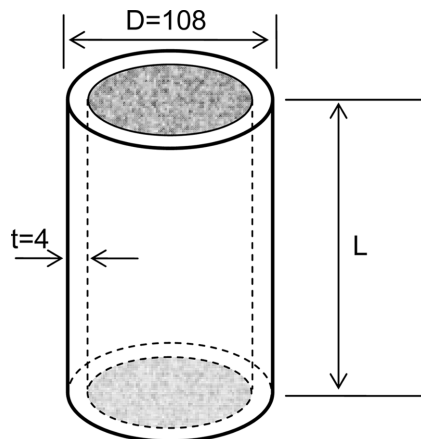


Fig. 2 Geometry of specimens used this study (unit: mm)

Table 2 CFST specimens and their abbreviations

Specimen	Length (mm)	$\bar{\lambda}$	Abbreviation for different loading schemes				
			LT-A	LT-B	LT-C	LT-D	LT-E
Short	324	0.14	SA	SB	SC	SD1, SD2	SE
Intermediate	1296	0.56	MA	MB	MC	MD1, MD2	ME
Long	1944	0.84	LA	LB	LC	LD1, LD2	LE

2.2 Test procedure

The tests were carried out in a 5000 kN capacity hydraulic compression machine at Fuzhou University, China. The test set up is shown in Fig. 3. The loading schemes of LT-A, -B, -C, -D1, -D2 and -E are compared in Fig. 4. Two LVDT transducers were used to measure the displacement between the top and bottom loading plates. Four pairs of strain gauges were attached to the steel tube surface at four positions (see P1-P4 in Fig. 3) along the perimeter at the mid-height of each short column to measure the vertical and circumferential strains. Additional strain gauge sets at the quarter height positions were

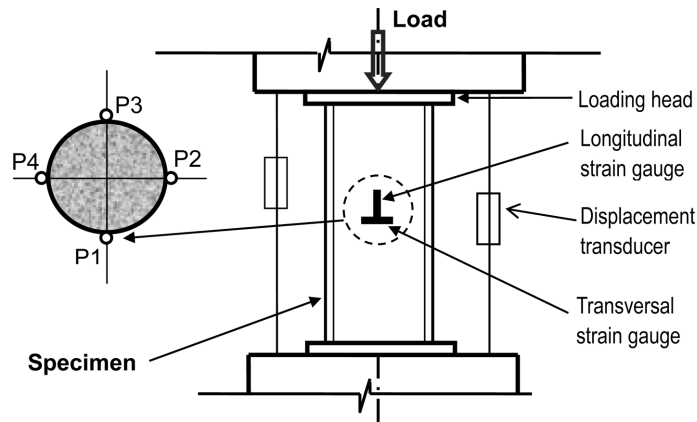


Fig. 3 Test setup for CFST columns under various loading schemes

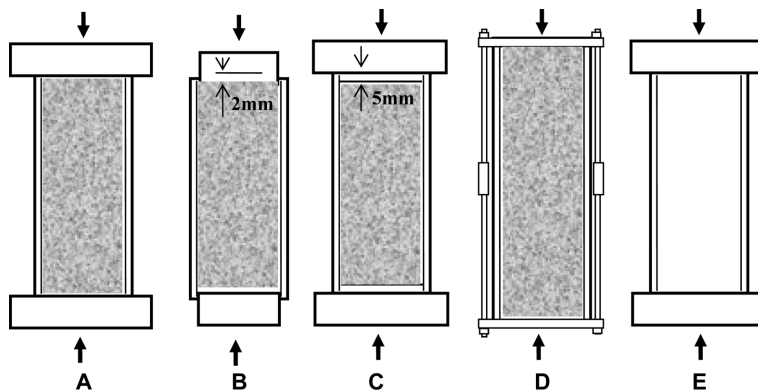


Fig. 4 Loading schemes used in this study

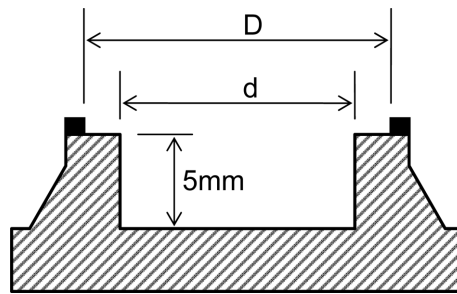


Fig. 5 Loading head designed for LT-C loading

also used on intermediate and long specimens.

Special loading heads were designed for LT-B and -C. For LT-B, a 2 mm end gap (see Fig. 3) was left to hold the 12 mm thick loading head in position. For LT-C, the specially made loading head diameter was 2 mm bigger than the tube to ensure full coverage of the steel tube but left a 5 mm gap to the concrete core (see Fig. 5). For LT-D, preloading was done by pre-stressing the tube by four steel bars. A strain gauge was attached on each bar to monitor the load applied matching the desired preloading ratio. Concrete was then filled after the forces in the bars were kept stable for 2 days.

The test loads were applied step by step to simulate a quasi-static loading condition. The ULs of the specimens were calculated roughly before testing. At each load step, the load was kept constant for at least 3 minutes to enable effective force introduction. For LT-A and -B, the step loads were initially set to 10% of the estimated ULs and halved after the yield of steel tube initiated (by observing the maximum axial strain readings). For LT-C, the step load was initially set to 10% of the estimated UL of the empty steel tube and switched to 10% of the UL of the composite column after the concrete core took action (by observing the appearance of stiffening phenomenon). For LT-D1 and -D2, the loads were applied the same as for LT-A and -B. For all the loading schemes, the incremental loads were tuned down when approaching to the ULs of the specimens. The loading process lasted until no more loads could be applied.

2.3 Test results and observations

2.3.1 Axial and lateral displacements

The axial load-displacement curves of the specimens are shown in Figs. 6-8. The history of lateral displacements at mid-height of intermediate and long specimens was also recorded (see Figs. 9 and 10).

2.3.1.1 Short columns

As shown in Fig. 6, the “SA” is significantly stiffer than “SB” at the beginning, but with larger axial displacements the opposite is evidenced. This result is different from the results presented in reference (Johansson *et al.* 2000), which stated that the difference is trivial. When the load is applied on the concrete core alone, the load introduction from the concrete core to the tube is achieved by the bonding between the tube and concrete core. The stiffness of the concrete core is obviously lower than that of the entire section. Therefore the concrete core should initially deform more in “SB” than in “SA”. However, the Poisson’s ratio induced confinement effect strengthens the column of LT-B more than LT-A in subsequent loading; finally the UL of “SB” slightly exceeds the UL of “SA”. It was evidenced that the specimen “SB” swelled out at the mid-height after testing together with crushing failure of concrete,

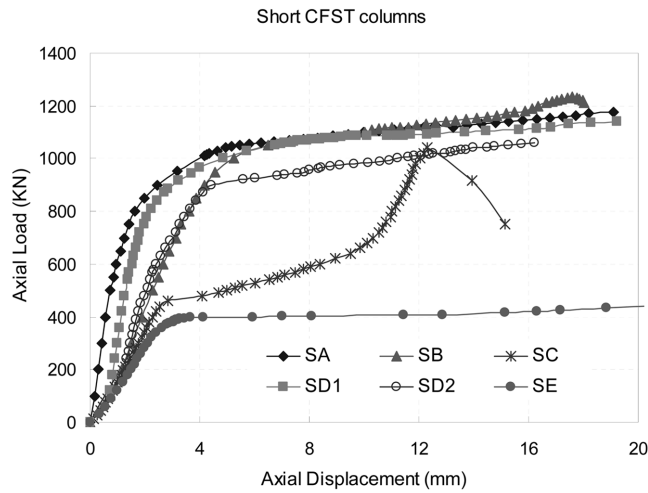


Fig. 6 The axial load-displacement curves of short CFST specimens

but “SA” did not. More explanations will be given in Section 2.3.2.

For the specimen “SC”, the load was applied initially on the tube only; no confinement effect could be expected. Its stiffness was as weak as that of the empty tube. The tube yielding started at a load of 448 kN, which is close to the UL of empty tube without considering strain hardening. The development of axial displacement accelerated until the load reached 675 kN when the axial deflection exceeded 10mm and the end gaps got closed so that the concrete core began to resist the axial load directly. This procedure corresponds to the sudden increase of the curve slope of “SC”. The behaviour of “SC” observed is similar to that in (Johansson *et al.* 2002).

It is also clear from Fig. 6 that low preloading ratio specimens (LT-D1) experience little UL reduction, but high preloading ratio specimens (LT-D2) do. Preloading reduces stiffness and advances the plastic response as the steel tube is pre-stressed. The axial displacements of the “SA”, “SB” and “SD1” were almost the same (about 8.1 mm) when the load was about 1070 kN.

2.3.1.2 Intermediate columns

The load-displacement curves of intermediate length CFST columns are shown in Fig. 7. The stiffness transformation between “MA” and “MB” is similar to that between “SA” and “SB”. However, the stiffness increase of “MB” over “MA” is much delayed. This indicates the confinement effect is considerably weaker for this length. Even though, this effect is still traceable as diagonal micro shear wrinkles were seen on the tube surface of specimen “MB” with further loading. Again, the UL of “MB” exceeds the UL of “MA”. The specimens finally failed by overall buckling. The tube yield load of “MC” (455 kN) was very close to the UL of “ME” (448 kN), the moment when the axial displacement started to increase quickly. The concrete core got involved in load resistance when the axial deflection reached 12 mm, which was slightly larger than the initial gap. This action can be inferred from the sudden increase of the slope of the curve “MC”.

The curve “MD1” is almost the same as “MA” except for an offset caused by preloading. But the UL and stiffness of “MD2” are much lower. Therefore slight preloading does not affect the UL too much. However, high preloading ratio (“MD2”) does. For both the short and intermediate specimens, the steel

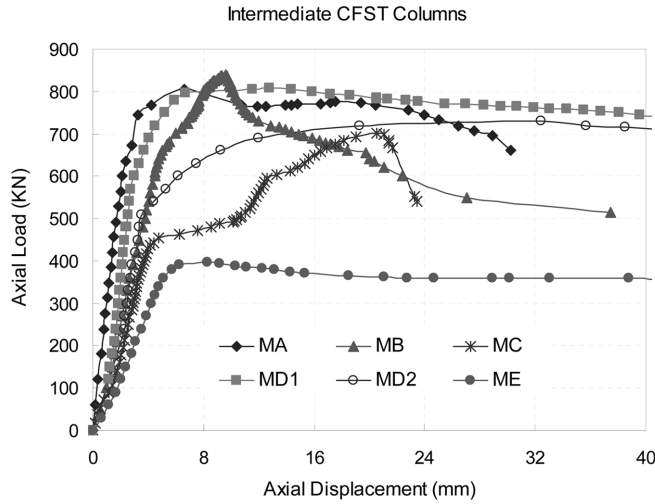


Fig. 7 The axial load-displacement curves of intermediate length CFST specimens

tubes subject to LT-C or -D2 yielded earlier than those subject to LT-A, -B or -D1. It was hard to control and keep a uniform stress distribution on the cross section of the specimens of this length that once the tube yielding occurs the lateral displacement increased rapidly leading to overall buckling.

2.3.1.3 Long columns

It seems that the type of the loading has a very limited influence on the load-displacement (both axial and lateral displacements, see Figs. 8 and 10) response in long specimens (except the LT-E and -C loadings with apparent early steel tube failure). This phenomenon agrees with the Saint-Venant's principle, which asserts that the contact due to support or load application become negligible at a

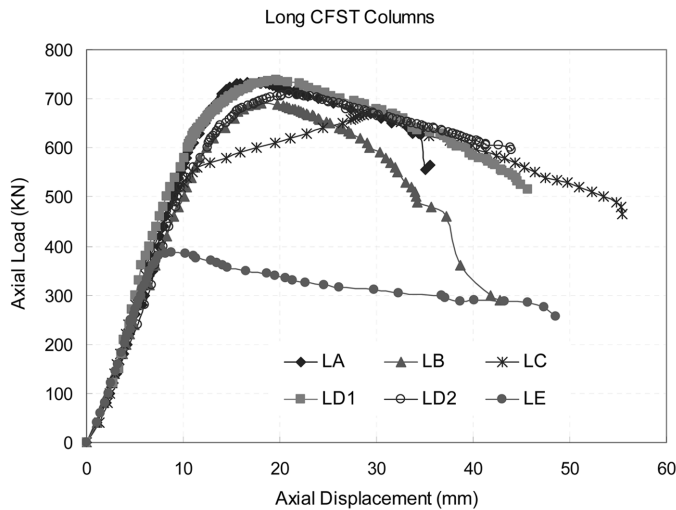


Fig. 8 The axial load-displacement curves of long CFST specimens

distance. The load can be introduced more effectively and evenly to the concrete core and surrounding steel tube in long CFST columns. The slenderness effect was so dominant that all the specimens failed by overall buckling. Indeed, although meticulous attention had been done to ensure concentric loading during tests, the long specimens started to bend soon. No swelling out was observed in the specimens. The relative lower UL of “LB” can be explained as the loss of stability before the fully load introduction from the concrete core to the steel tube. The significant difference of structural response between the short and long columns shows that the UL of a slender specimen is determined by its stability instead of its cross section strength.

2.3.1.4 Summary

It is evident from Figs. 6-8 that shorter specimens have higher UL than longer ones for the same loading scheme. Short specimens fail by local buckling, but intermediate and long specimens fail by overall buckling. The overall buckling can be inferred from the quick increase of lateral displacements when the load is approaching the UL, as shown in Figs. 9 and 10.

For short specimens, the strengthening effect of LT-B loading helps to gain some increase in the UL. However, overall buckling failure might occur before the strengthening effect is fully developed in long columns. This loading scheme experiences much sharper drop of residual strength once the peak load is reached.

The LT-C scheme is actually a special case of LT-D scheme with extremely high preloading ratio. Low preloading ratio (LT-D1) does not reduce the UL much. But high preloading ratio (LT-D2 and LT-C) does. This agrees with (Liew *et al.* 2009) in that high preloading ratio could cause a reduction of axial capacity of more than 20%. However, different from (Liew *et al.* 2009), which concluded that preloading much affected intermediate and slender columns, the UL reduction was not significant in this research for long, *i.e.*, slender, specimens.

The axial strains at peak loads of the three LT-C specimens were almost the same as those of the corresponding LT-D2 loadings, which (calculated from the axial displacements) were 3.70%, 1.54% and 1.54% for short, intermediate and long specimens, respectively. The difference of these strains

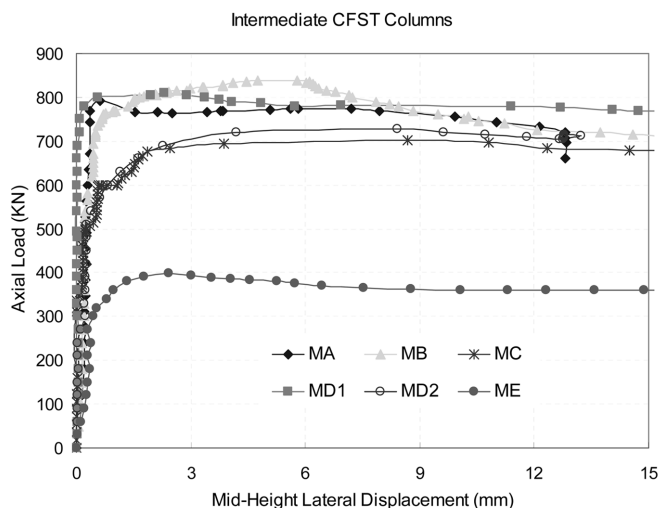


Fig. 9 The axial load and lateral-displacement curves of intermediate CFST specimens at the mid-height of the column

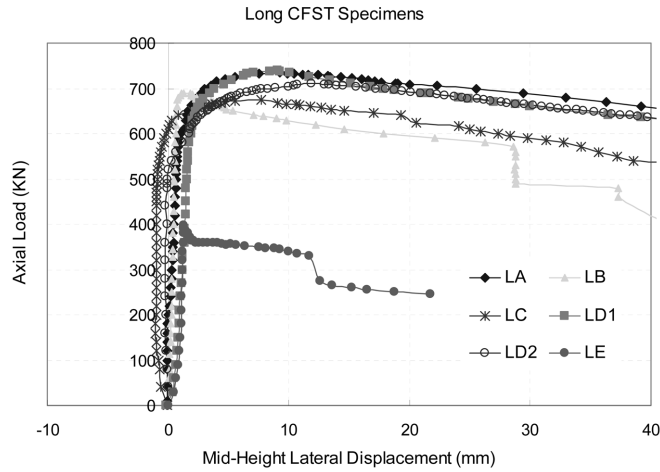


Fig. 10 The axial load and lateral-displacement curves of long CFST specimens at the mid-height of the column

indicates the failure mechanisms (local buckling or overall buckling) of the specimens of different lengths. However, the UL of LT-D2 is slightly higher than that of LT-C.

Comparing the LT-C load-displacement curves of different lengths, the structural response can be outlined as: steel tube yielding when the UL of the steel tube is reached → accelerated deformation → concrete core in action → increased stiffness → peak strength reached → sudden failure. The relative lower UL and the sudden drop of load resistance later on make clear the risk of brittle failure (, especially for short columns), and therefore should be avoided in engineering practice. If this loading condition is caused by shrinkage of concrete, then filling the gap in time is necessary. Some researchers suggest using expanding agent in concrete to reduce shrinkage. However, its long term performance in the dry sealed tube is still not clear.

2.3.2 Confinement effects

When a load is applied on the entire section on a short CFST column (LT-A), at the initial stage the Poisson's ratio of steel exceeds that of concrete, so the concrete and steel resist the load separately. Micro-cracking in concrete increases the Poisson's ratio of concrete and surpasses that of steel at about 0.2% of strain (Knowles *et al.* 1969). Quick volumetric dilation enables the confinement effect. Although this confinement effect reduces the axial load capacity of steel tube due to bi-axial stressing, the resultant load capacity of the column is enhanced. This effect develops and increases more quickly in LT-B than in LT-A.

In the intermediate and long CFST specimens the load can be more effectively introduced into the entire section. Furthermore, slender specimens tend to develop lateral displacement leading to overall buckling so that the confinement effect is insignificant. Therefore different loading schemes cause very little difference on the structural response.

The confinement effect is one of the key characteristics in short CFST columns. This effect in some extent can be estimated from the nominal composite Poisson's ratio of CFST, $\bar{\nu}_c$, defined as (Han *et al.* 2011)

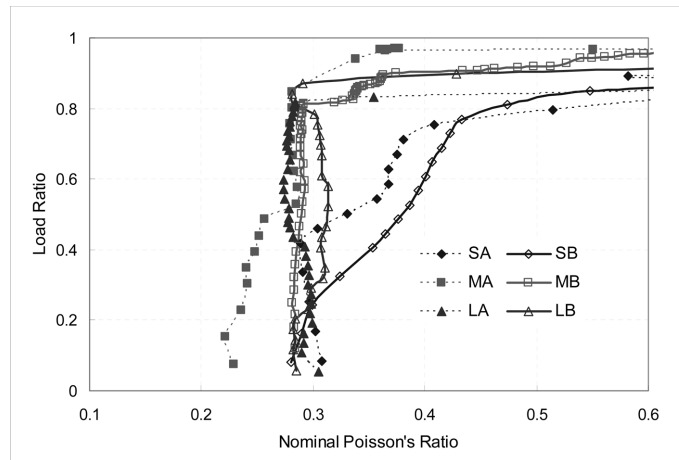


Fig. 11 Comparison of the nominal Poisson's ratio in specimens subject to the LT-A and -B loading

$$\bar{\nu}_c = \left| \frac{\text{circumferential strain}}{\text{axial strain}} \right| \quad (2)$$

The confinement effect can be regarded as negligible if $\bar{\nu}_c$ is close to the Poisson's ratio of steel. Among all types of the loading schemes, LT-B, when the load is applied on the concrete core, must activate the most significant confinement effect. LT-C should have the least confinement effect. However, as stated above, this loading condition must be avoided in engineering practice. Therefore, only the $\bar{\nu}_c$ of LT-A and -B at the mid-height of the specimens are compared (see Fig. 11).

As shown in Fig. 11, the nominal Poisson's ratios of the long and intermediate specimens do not change much until the load ratio, defined as load over UL, reaches 0.8. However, for the short specimens, significant increase of $\bar{\nu}_c$ appears at a load ratio of about 25%. This difference of $\bar{\nu}_c$ gives further collateral evidence that long specimens failed by overall buckling while short specimens failed by squashing. It also supports the EC4 in that the confinement effect is considered only when $\lambda \leq 0.5$. The λ of the intermediate length group, which is about 0.5, borders on this limit.

2.3.3 The effect of various loading schemes on the UL of CFST columns

The relationship between the UL and the slenderness parameter (L/D) of the specimens tested is summarized in Fig. 12. In this figure, the nominal UL of each specimen is defined as the ratio of the UL over the UL of LT-A. Obviously, the load capacity of LT-C is the lowest among all loading schemes. Excessive pre-stressing also reduces the load capacity of CFST columns. However, slight pre-stressing does not affect the UL too much. This agrees with the conclusion in (Liew *et al.* 2009).

3. Simplified methods for predicting the UL of CFST columns

The design of an engineering structure must ensure that, under the worst of feasible loading conditions, the structure is safe. In other words, in the prediction of the UL of CFST columns, no partial safety factors should be used.

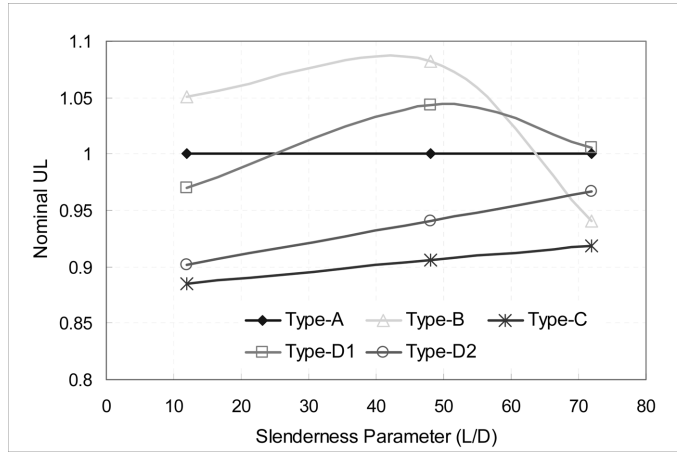


Fig. 12 The influence of loading schemes on the ultimate load capacity of CFST specimens

3.1 The UL for the LT-A loading N_u^A

In the EC4, the UL of concentrically loaded circular CFST columns is calculated as

$$N_u^A = \chi N_{pl,Rk} \quad (3)$$

where χ , which is derived analytically from the stress at an admissible deflection at mid-height (Liew *et al.* 2009), is used to reduce the plastic compressive resistance of the cross section, $N_{pl,Rk}$, for slender columns; and

$$\begin{aligned} N_{pl,Rk} &= \eta_2 A_a f_y + \left(1 + \eta_1 \frac{t f_y}{D f_{ck}}\right) A_c f_{ck} = \eta_2 \frac{A_a f_y}{N_a} + \frac{A_c f_{ck}}{N_c} + \eta_1 \frac{t}{D} (f_y A_c) \\ &= \eta_2 N_a + N_c + \eta_1 \frac{t}{D} (f_y A_c) \end{aligned} \quad (4a)$$

where

$$\begin{cases} \eta_1 = 4.9 - 18.5 \bar{\lambda} + 17 \bar{\lambda}^2 \geq 0 \\ \eta_2 = 0.25(3 + 2 \bar{\lambda}) \leq 1 \end{cases} \quad (4b)$$

where η_1 and η_2 are factors considering confinement effect when the relative slenderness $\bar{\lambda} \leq 0.5$. Both η_1 and η_2 are assumed to be functions of λ only. The η_2 , which considers the reduction of the axial strength of the tube subject to circumferential stretching, changes between 0.75 (when $\lambda = 0$) and 1 (when $\lambda = 0.5$). The η_1 , which accounts for the interaction between the tube and the concrete core, changes between 4.9 and 0. The effect of this interaction is further corrected by the cross section parameters, t/D , and the relative strength of steel and concrete, f_y/f_{ck} .

In the Chinese CECS, the UL of concentrically loaded circular CFST columns is calculated as

$$N_u^A = \varphi_t N_0 \quad (5)$$

where the φ_l is the reduction factor considering the slenderness influence, changes between 1 (short) and 0.54 (slender); and N_0 is the UL of the CFST column of short length, which is a function of confinement factor, ξ , defined as the cross sectional plastic capacity ratio of the steel over the concrete core. The interaction between the tube and the concrete core, including confinement effect, is treated equally without considering the different mechanisms behind.

$$N_0 = A_c f_{ck} (1 + \sqrt{\xi} + \xi) = A_a f_y + A_c f_{ck} + \sqrt{(A_c f_{ck})(A_a f_y)} = N_a + N_c + \sqrt{N_c N_a} \quad (6)$$

It is apparent that the concepts behind the EC4 and the Chinese CECS are different. Although the CECS employs less subtle calibration than the EC4 method, the CECS predictions are very good as shown in Table 3. It can also be seen from this table that the EC4 method underestimates the confinement effect in CFST columns. It is hard to identify which method is better only by this limited comparison, but they are only applicable to the LT-A loading condition.

3.2 The UL of the LT-B loading, N_u^B

The confinement effect makes the N_u^B larger than N_u^A of short CFST columns. However, experimental results (see Table 4) show that the difference is within 10% of N_u^A . Due to limited experiment data and unavoidable experimental error, it is hard to establish the relationship between N_u^B and N_u^A .

FE analyses (Starossek *et al.* 2009) found that the maximum longitudinal stress of steel at ultimate load of LT-B was approximately 60% of the yield strength. A design proposal was derived (Starossek *et al.* 2009) subsequently based on tests for this type of loading as

$$N_{u,Rd}^B = (f_{ck} + 35) \frac{1}{\gamma_c} \sqrt{\frac{A_c}{A_1}} A_1 + 0.6 A_a f_y \quad (7)$$

where A_1 is the area below the loading plate (personal contact). The unit material safety factor, γ_c , is used to calculate the UL. When Eq. (7) is used to predict the UL of CFST columns, the γ_c is discarded. However, the predictions (see Table 4) exhibit sparse distribution of error. The slenderness influence

Table 3 The prediction of the UL of specimens subject to the LT-A loading

Specimen	N_{test} (kN)	L/D	CECS (1992)					EC4 (2004)					
			N_0 (kN)	φ_l^{test}	φ_l^{calc}	N_{calc} (KN)	Err (%)	$\bar{\lambda}$	N_0 (KN)	χ^{test}	φ^{calc}	N_{calc} (kN)	Err (%)
SA	1175	3		1.009	1.000	1174	-0.09	0.135	969	1.213	1.000	969	-17.53
MA	774	12	1174	0.696	0.674	792	+2.33	0.539	784	0.987	0.912	715	-7.62
LA	735	18		0.626	0.570	669	-8.98	0.808		0.938	0.791	620	-15.65

Note: $\varphi_l^{test} = N_0/N_{test}$, $\chi^{test} = N_{pl,R}/N_{test}$, $N_0 = N_{pl,R}$, Err = $N_{calc}/N_{test} - 1$

Table 4 Comparison of UL of columns subject to the LT-A and -B loading (unit: kN)

Specimen	$N_{u,test}^A$ (1)	$N_{u,test}^B$ (2)	$N_{u,calc}^B$ (3)	(1) - (2)	(3) - (2)
SB	1175	1235		-60	-352
MB	774	839	883	-65	-44
LB	735	690		45	-193

Note: (3) is calculated using Eq. (7)

and confinement effects can hardly be identified in Eq. (7).

3.3 The UL of the LT-C and -D loading

Seen from Figs. 6-9, the ULs of the LT-C and -D2 specimens are closed to each other. However, the early yielding of the tube and the tendency of brittle failure makes it necessary to avoid LT-C loading as a mandatory requirement in engineering practice. So, the UL of the LT-C loading is not discussed here.

Liew and Xiong (2009) extended the EC4 simplified method to preloaded CFST columns by replacing the slenderness reduction factor, χ , with χ_{pre} to account for the preloading effect for short or slightly preloaded CFST columns. That is

$$\chi_{pre} = \frac{1}{\varphi_{pre} + \sqrt{\varphi_{pre}^2 - \bar{\lambda}^2}} \quad (8)$$

where

$$\varphi_{pre} = 0.5[1 + 0.21(\xi_{pre}\bar{\lambda} - 0.2) + \bar{\lambda}^2] \quad (9)$$

with the ξ_{pre} be the preloading effect factor defined as

$$\xi_{pre} = \frac{1 - N_{pre}/(\chi N_{pl,Rk})}{1 - N_{pre}/(\chi_a N_{a,pl,Rk})} \geq 1 \quad (10)$$

where N_{pre} is the preloading applied, and $\chi N_{pl,Rk}$ and $\chi_a N_{a,pl,Rk}$ are the reduced plastic resistance of the composite column and the steel tube respectively.

However, from the comparison of the test results and the predictions using this method listed in Table 5 it can be seen that this method overestimates the preloading influence.

3.4 Development of a generalized UL prediction method for circular CFST columns subject to various loading conditions

As illustrated above, there is still lack of a generalized prediction method for predicting the ULs of CFST columns subject to various loading conditions. Therefore, a new prediction method, which is extended from the CECS method, is developed in this study. It is assumed that prediction can be expressed in a unified form as shown in Eq. (11).

$$N_u^k = \varphi_l(\alpha_1^k N_a + \alpha_2^k N_c + \alpha_3^k \sqrt{(\alpha_1^k N_a)(\alpha_2^k N_c)}) \quad (11)$$

where $k = A, B, C$ or D , represents the type of loading condition; The parameters, α_i^k ($i = 1, 2, 3$), which use the advantages of both the EC4 and the CECS methods, are used to calibrate the prediction.

3.4.1 LT-A

For the LT-A, let $\alpha_1^A = \alpha_2^A = \alpha_3^A = 1$, then the CECS method is recovered. The EC4 method can also be recovered by setting $\varphi_l = \chi$, $\alpha_1^A = \eta_2$, $\alpha_2^A = 1 + \eta_1(t/D)(f_y/f_{ck})$, and $\alpha_3^A = 0$.

3.4.2 LT-B

For the LT-B, the change of the resistance of the steel tube is neglected, i.e., $\alpha_1^B = 1$. If the

Table 5 Comparison of UL of CFST columns subject to the LT-D loading using the method given in (Liew *et al.* 2009)

	Specimen	Dimension $D \times t \times L$ (mm)	f_y (MPa)	f_{ck} (MPa)	β^b	N_{test} (kN)	N_{calc} (kN)	$(N_{pre}/N_{test}) - 1$
Liew <i>et al.</i> (2009) ^a	S-40-30P	219×6.3×708	300	37	0.252	3677	3048	-17.11%
	S-100-30P		300	107	0.250	4667	5216	11.75%
	I-40-30P	219×6.3×1728	405	44	0.299	3648	3031	-16.93%
	I-100-30P		405	113	0.305	5278	4927	-6.65%
	I-130-40P		405	139	0.380	5437	5568	2.41%
	L-40-30P	219×6.3×3078	393	49	0.306	3160	2776	-12.15%
	L-100-30P		393	111	0.310	4580	4269	-6.78%
	L-130-40P		393	125	0.399	4827	4441	-8.00%
SD1	108×4×324		336	44	0.250	1140	969	-14.96%
SD2		336	44	0.540	1060	969	-8.57%	
This study	MD1	108×4×1296	336	44	0.200	809	700	-13.42%
	MD2		336	44	0.432	729	664	-8.93%
	LD1	108×4×1944	336	44	0.166	738	677	-8.26%
	LD2		336	44	0.359	710	614	-13.55%
Standard Deviation								7.77%

^athe Young’s Modulus of steel is assumed to be 210 GPa

^bthe preloading ratio in (Liew *et al.*, 2009) has a different meaning which is defined as $\beta = N_{pre}/N_{a,ck}$. Therefore, the preloading ratios in (Liew *et al.*, 2009) and this study are related as $\beta_{Liew} = \chi_a \beta$.

confinement strengthening effect is assumed to be linearly related to $\bar{\lambda}$, then $\alpha_2^B = 1.5 - \bar{\lambda}$, which reduces to 1 when $\bar{\lambda} = 0.5$. The α_3^B can be determined statistically. Based on the current experiment results of SB, MB and LB, the α_3^B can be interpolated linearly from $\bar{\lambda}$ as (see Fig. 13)

$$\alpha_3 = 1.3794\bar{\lambda} + 0.5182 \tag{12}$$

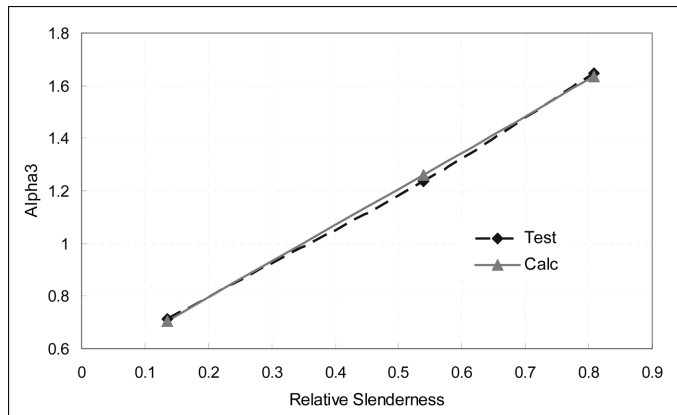


Fig. 13 The linear approximation of the relationship between the $\bar{\lambda}$ and the α_3^B

Table 6 The prediction of the ultimate load capacity of CFST columns subject to the LT-B loading using proposed generalized method

Specimen	Dimension $D \times t \times L$ (mm)	f_{ck}	f_y	φ_l	α_2^B	α_3^B	N_t	N_u^B	N_u^B/N_t
SB	108×4×324	43.9	336	1.000	1.365	0.704	1235	1229	0.995
MB	108×4×1296	43.9	336	0.675	0.961	1.261	839	844	1.006
LB	108×4×1944	43.9	336	0.570	0.692	1.633	690	687	0.995
Standard deviation									0.006
Mean									0.999

Note: The unit of f_{ck} and f_y is MPa; The unit of N_t and N_u^B is kN.

The comparison of a few test results and the predictions using this assumption given in Table 6 shows the accuracy of these parameters. However, only the very limit test results in this research are used, further study on this type of loading condition is necessary to obtain more comprehensive calibration parameters.

3.4.3 LT-C

No strengthening effect can be obtained by this type of loading, therefore, $\alpha_1^C = 1$ and $\alpha_2^C = \alpha_3^C = 0$. However, if the column is short, the shrinkage of concrete inside the steel column is ignorable as concrete hardens under a sealed condition inside the steel (JSCE 2006).

3.4.4 LT-D

This type of loading is similar to LT-A loading except the steel tube is preloaded. Comparing with the UL of LT-A, the reduction of the UL due to preloading is summarized in Fig. 14. The average relationship between the reduction factor, r , and the preloading ratio, β , can be approximated as

$$r \approx 1.067 - 0.241\beta \leq 1 \quad (13)$$

Hence, $\alpha_i^D = r\alpha_i^A$. Both this study and (Liew *et al.* 2009) show that there is very little strength reduction when the preloading ratio is low, therefore, $r = 1$ when β is low. Using this approximation, the

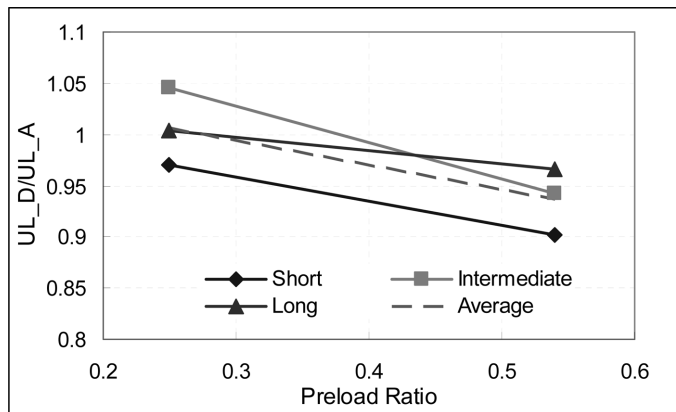


Fig. 14 The ratio of N_u^D/N_u^A reduces with the increase of preloading ratio

Table 7 The prediction of the ultimate load capacity of CFST columns subject to the LT-D loading using the proposed generalized method

	Specimen	Dimension $D \times t \times L$ (mm)	f_{ck}	f_y	β	φ_l	r	N_t	N_u^D	N_u^D/N_t
Zha (1996)	ZI1-1	133×4.5×1862	33.76	325	0	0.636	1.000	895	947	1.058
	ZI2		33.76	325	0.305	0.636	0.993	882	941	1.067
	ZI3		33.76	325	0.436	0.636	0.962	715	911	1.274
	ZL1-1	133×4.5×2973	33.76	325	0	0.526	1.000	743	782	1.053
	ZL2		33.76	325	0.311	0.526	0.992	748	776	1.038
	ZL3		33.76	325	0.498	0.526	0.947	800	741	0.926
Han <i>et al.</i> (2003)	HS1-1	120×2.65×360	16.08	340	0	1.000	1.000	640	733	1.145
	HS1-2		16.08	340	0.499	1.000	0.947	664	694	1.045
	HS2-1		28.80	340	0	1.000	1.000	816	944	1.156
	HS2-2	28.80	340	0.499	1.000	0.947	812	893	1.100	
	HI1-1	120×2.65×1400	28.80	340	0	0.682	1.000	769	643	0.836
	HI1-2		28.80	340	0.499	0.682	0.947	730	609	0.834
This Study	SD1	108×4×324	43.92	336	0.250	1.000	1.000	1140	1173	1.029
	SD2		43.92	336	0.540	1.000	0.937	1060	1099	1.036
	MD1	108×4×1296	43.92	336	0.250	0.675	1.000	809	791	0.978
	MD2		43.92	336	0.540	0.675	0.937	729	741	1.017
	LD1	108×4×1944	43.92	336	0.250	0.570	1.000	738	668	0.905
	LD2		43.92	336	0.540	0.570	0.937	710	626	0.882
Liew <i>et al.</i> (2009)	S-40-30P	219×6.3×708	37.00	300	0.252	1.000	1.000	3677	3749	1.020
	I-40-30P	219×6.3×1728	44.00	405	0.324	0.773	0.989	3648	3639	0.997
	L-40-30P	219×6.3×3078	49.00	393	0.417	0.635	0.967	3160	3033	0.960
Standard deviation									0.106	
Mean									1.017	
Liew <i>et al.</i> (2009)	S-100-0P	219×6.3×708	108.00	300	0.000	1.000	1.000	5410	7009	1.296
	S-100-30P	219×6.3×708	107.00	300	0.250	1.000	1.000	4667	6966	1.493
	I-100-0P	219×6.3×1728	99.00	405	0.000	0.773	1.000	4977	5714	1.148
	I-100-30P	219×6.3×1728	113.00	405	0.331	0.773	0.987	5278	6123	1.160
	I-130-40P	219×6.3×1728	139.00	405	0.412	0.773	0.968	5437	6859	1.262
	L-100-0P	219×6.3×3078	100.00	393	0.000	0.635	1.000	4204	4669	1.111
	L-100-30P	219×6.3×3078	111.00	393	0.422	0.635	0.965	4580	4810	1.050
	L-130-40P	219×6.3×3078	125.00	393	0.543	0.635	0.936	4827	5033	1.043

Note: 1. f_{ck} is calculate from the cubic strength as $f_{ck} = 0.8f_{cubes}$, 2. f_{ck} and f_y are in MPa; N_t , and N_u^D are in kN, 3. The β for Liew *et al.* (2009) is calculated by $\beta = \beta_{Liew} \chi_a$.

ULs of CFST specimens by Zha (1996), Han *et al.* (2003), Liew *et al.* (2009) and those tested in this research are calculated and listed in Table 7. It can be seen the predictions are very good when the compressive strength of concrete is not too high ($f_{ck} \leq 50$ MPa). For high strength concrete, the CECS method tends to overestimate the N_0 , consequently, the N_u^D is overestimated. This is due to the CECS method validity only for characteristic strength of concrete in the range between 30 MPa and 80 MPa (Kuranovas *et al.*, 2009). The concrete strength in the EC4 method is confined to a certain limit too

(Goode *et al.* 2008).

4. Conclusions

An experimental comparative study on a total of eighteen short, intermediate and long circular CFST columns subject to various concentric axial loading schemes have been carried out. The loads were applied on the entire section (LT-A), the concrete core only (LT-B), the steel tube only (LT-C), or on the entire section with two different preloading ratios (LT-D1 and -D2). For a complete comparison, three empty steel tubes were also tested (LT-E).

The test results show that the confinement effect is significant in short CFST columns, hence strengthening the columns. The LT-B loading has the most significant confinement effect of all considered types of loading. However, high slenderness ratio makes the CFST column tend to fail by overall buckling. Hence, there is little chance to develop the confinement effect. The investigation on the nominal Poisson's ratio of the composite specimens shows that the contribution of confinement effect is negligible in the intermediate ($\bar{\lambda} \approx 0.50$) and long ($\bar{\lambda} = 0.84$) specimens. This study supports the EC4 method in that relative slenderness of 0.5 is a reasonable limit for consideration of confinement effect in circular CFST columns.

Slight preloading has little influence on the structural performance, but over-preloading does reduce the load capacity. Therefore, too many storeys of ascending of building skeleton before filling of concrete should be avoided.

Compared with the LT-A, -B, and -D loading schemes, the LT-C loading exhibits least load resistance and therefore should be avoided as a mandatory requirement in construction.

In order to evaluate the ultimate load capacity of CFST columns under various loading conditions, a generalized UL predicting method is developed. This formulation uses three parameters, adopting the concepts behind the CECS and the EC4 methods and the distribution of the test results obtained from experimental study, to calibrate the accuracy of prediction. It is shown that the ultimate load capacity predictions by this method agree well with test results.

However, due to lack of test data for a comprehensive peer-to-peer comparative study on the ultimate load capacity of CFST columns subject to various loading conditions, such as LT-B, further research is needed.

Acknowledgement

The authors would like to thank Professor Zlatko Šavor of the University of Zagreb, Croatia for his careful check of this manuscript.

References

- American Concrete Institute (ACI). (1999), *Building code requirements for structural concrete and commentary*, ACI 318-99/R-99. Farmington Hills.
- American Institute of Steel Construction (AISC). (2005), "*Manual for structural steel buildings: Load and Resistance Factor Design (LRFD)*", Chicago.

- Australia Standards (AS). (1998), “AS4100 Steel structures”. Sydney: Standards Australia.
- Bahrami, A., Badaruzzaman, W.H.W. and Osman, S.A. (2011), “Nonlinear analysis of concrete-filled steel composite columns subjected to axial loading”, *Struct. Eng. Mech., An Int'l Journal*, **39**(3), 383-398.
- CECS 28:90. (1992), “Specification for design and construction of concrete-filled steel tube structures”, China Planning Press. (in Chinese)
- Chen, B.C. and Wang, T.L. (2009), “Overview of Concrete Filled Steel Tube Arch Bridges in China”, DOI: 10.1061/(ASCE) 1084-0680, 14:2 (70).
- China Building Material Industry Standard (JCJ). (1989), “Design and Construction Specifications for concrete filled steel tube structures (JCJ01-89)”, Tongji University Press, China. (in Chinese)
- China Electric Power Industry Standard (DL/T). (1999), “Design Specifications for Steel-Concrete Composite Structures (DL/T5085-1999)”, China Electric Power Press. (in Chinese)
- Cai, S. (1989), “Calculation and application of concrete-filled steel tubes”, China Architecture & Building Press, Beijing. (in Chinese)
- Dai, X. and Lam, D. (2010), “Axial compressive behaviour of stub concrete-filled columns with elliptical stainless steel hollow sections”, *Steel and Composite Structures, An Int'l Journal*, **10**(6), 517-539.
- Eurocode 4 (EC4). (2004), “Design of composite steel and concrete structures, Part 1.1: General rules and rules for buildings”. Brussels: Commission of European Communities.
- GB 50017. (2003), “Code for Design of Steel Structures”, 1st Ed., Ministry of Construction of China, Beijing, China. (in Chinese)
- Goode, C.D. and Lam, D. (2008), “Concrete-filled steel tube columns - tests compared with Eurocode 4”, In: *Composite Construction VI*, July 20-24, Devil's Thumb Ranch, Colorado, USA.
- Gourley, B.C., Tort, C., Denavit, M.D., Schiller, P.H. and Hajjar, J.F. (2008), NSEL Report: “A Synopsis of Studies of the Monotonic and Cyclic Behaviour of Concrete-Filled Steel Tube Members, Connections, and Frames”, Report No. NSEL-008.
- Gupta, P.K., Sarda, S.M. and Kumar, M.S. (2007), “Experimental and computational study of concrete filled steel tube columns under axial loads”, *J. Constr. Steel Res.*, **63**(2), 182-193.
- Han, L.H. and Yao, G.H. (2003), “Behaviour of concrete-filled hollow structural steel (HSS) columns with pre-load on the steel tubes”, *J. Constr. Steel Res.*, **59**(11), 1455-1475.
- Han, L.H., Zheng, L.Q., He, S.H. and Tao, Z. (2011), “Tests on curved concrete filled steel tube members subjected to axial compression”, *J. Constr. Steel Res.*, doi:10.1016/j.jcsr.2011.01.012.
- Hybrid Structure Series 02 (JSCE). (2006), “Guidelines for performance verification of steel-concrete hybrid structures”, Committee on Hybrid Structures.
- Johansson, M., Cleason, C., Gylltoft, K. and Akesson, M. (2000), “Structural behaviour of circular composite columns under various means of load application”, *Proceeding of 6th ASCCS Conference*, Los Angeles, USA.
- Johansson, M. and Gylltoft, K. (2002), “Mechanical behaviour of circular steel-concrete composite stub columns”, *J. Struct. Eng., ASCE*, **128**(8), 1073-1081.
- Knowles, R.B. and Park, R. (1969), “Strength of Concrete Filled Steel Tube Columns,” *Journal of the Structural Division, ASCE*, **95**(ST12), 2565-2587.
- Kuranovas, A., Goode, D., Kvedaras, A.K. and Zhong, S.T. (2009), “Load-bearing capacity of concrete-filled steel columns”, *Journal of Civil Engineering and Management*, **15**(1), 21-33.
- Liew, J.Y.R. and Xiong, D.X. (2009), “Effect of preload on the axial capacity of concrete-filled composite columns”, *J. Constr. Steel Res.*, **65**, 709-722.
- Manojkumar, V.C., Matur, C.N. and Kulkarni, S.M. (2010), “Axial strength of circular concrete-filled steel tube columns - DOE approach”, *J. Constr. Steel Res.*, **66**, 1248-1260.
- O’Shea, M.D. and Bridge, R.Q. (2000), “Design of circular thin-walled concrete filled steel tubes”, *J. Struct. Eng., ASCE*, **126**(11), 1295-1303.
- O’Shea, M.D. and Bridge, R.Q. (1997), “Tests on circular thin-walled steel tubes filled with medium and high strength concrete”, Report No. R755, School of Civil Engineering, University of Sydney, Australia.
- Starossek, U. and Falah, N. (2008), “The interaction of steel tube and concrete core in concrete-filled steel tube columns”, in *Tube Structures XII*, Shen, Chen & Zhao (eds), Taylor & Francis Group, London, ISBN 978-0-415-46853-4, 75-84.
- Wang, Y., Zhang, S. and Guo, L. (2005), “Influence of load conditions on mechanical behaviour of CFST stub

- columns subjected to axial compression”, *Journal of Harbin Institute of Technology*, **37**(1), 40-44.
- Xiamuxi, A. and Hasegawa, A. (2010), “Load-sharing ratio analysis of reinforced concrete filled tubular steel columns”, *Steel and Composite Structures, An Int'l Journal*, **12**(6), 523-540.
- Zha, X.X. (1996), “Investigation on the behaviour of concrete filled steel tube compression-bending-torsion members under the initial stress”, *PhD thesis*, Harbin University of C.E. Architecture.
- Zhu, W.C., Ling, L., Tang, C.A., Kang, Y.M. and Xie, L.M. (2012), “The 3D-numerical simulation on failure process of concrete-filled tubular (CFT) stub columns under uniaxial compression”, *Computers and Concrete, An Int'l Journal*, **9**(4), 257-273.

Nomenclature

α_i^k	Parameters used in the generalized UL prediction method, $i=1,2$ or 3 and k is the loading condition
β	Preloading ratio, defined as $\beta = \sigma_0/f_y$
β_{Liew}	Preloading ratio used in (Liew <i>et al.</i> 2009), defined as $\beta_{Liew} = N_{pre}/N_{a,cr}$
φ_l	Reduction factor considering the slenderness influence, $\begin{cases} \varphi_l = 1 - 0.115 \sqrt{l_e/D - 4} & \text{for } (l_e/D) > 4 \\ \varphi_l = 1 & \text{for } (l_e/D) \leq 4 \end{cases}$ (where $l_e/D \leq 20$)
γ_c	Partial safety factor of concrete for ULS (see Eq. (7))
χ	Slenderness reduction factor for CFST, $\chi = 1/(\phi + \sqrt{\phi^2 - \bar{\lambda}^2})$, with $\phi = 0.5[1 + 0.21(\bar{\lambda} - 0.2) + \bar{\lambda}^2]$
χ_a	Slenderness reduction factor for the steel tube, $\chi_a = 1/(\varphi_a + \sqrt{\varphi_a^2 - \lambda_a^2})$, where $\varphi_a = 0.5[1 - 0.21(\lambda_a - 0.2) + \lambda_a^2]$ and $\lambda_a = \sqrt{A_a f_y / (\pi^2 E_a I_a / l^2)}$
χ_{pre}	Slenderness reduction factor for CFST column with pre-stressing (Liew <i>et al.</i> , 2009)
ξ	Confinement factor, defined as $\xi = (f_y A_a)/(f_{ck} A_c)$
ξ_{pre}	Pre-stressing effect reduction factor (Liew <i>et al.</i> 2009)
$\bar{\lambda}$	Relative slenderness, defined as $\bar{\lambda} = \sqrt{N_{pl,R}/N_{cr}}$
$\bar{\nu}_c$	Nominal Poisson's ratio of CFST composite column
σ_0	Preloading stress in the steel tube
η_1	Confinement effect parameter, $\eta_1 = 4.9 - 18.5 \bar{\lambda} + 17 \bar{\lambda}^2 \geq 0$
η_2	Confinement effect parameter, $\eta_2 = 0.25(3 + 2 \bar{\lambda}) \leq 1$
A_a	Cross sectional area of the steel tube
A_c	Cross sectional area of the concrete core
A_1	Area below the loading head for the LT-B loading (see Eq. (7))
D	Outer diameter of the cross section of circular CFST column
E_a	Young's modulus of steel
E_c	Young's modulus of concrete
E_{cm}	Secant modulus of elasticity of concrete, $E_{cm} = 22 \times [(f_{ck} + 8)/10]^{0.3}$
f_{ck}	Cylindrical characteristic strength of concrete
f_y	Yield strength of steel
I_a	Area moment of inertia of the steel tube

I_c	Area moment of inertia of the concrete core
k	Type of loading condition, $k = A, B, C$ or D
L, l	Length of CFST columns
l_e	Effective length of the column, which is determined by the supporting conditions
N_0	UL of short CFST column, $N_0 = f_{ck}A_c(1 + \sqrt{\xi} + \xi)$
N_a	Plastic load capacity of the cross section of the steel tube, $N_a = A_a f_y$
N_c	Plastic load capacity of the cross section of the concrete core, $N_c = A_c f_{ck}$
N_{cr}	Euler buckling load of the composite column: $N_{cr} = \pi^2(EI)_e/l_e^2$, with $(EI)_e = E_a I_a + 0.6E_{cm}I_c$
$N_{a, pl, Rk}$	Characteristic cross-sectional plastic resistance of the steel tube, $N_{a, pl, Rk} = A_a f_y$
$N_{pl, Rk}$	Plastic resistance of cross section to axial load, $N_{pl, Rk} = A_a f_y + A_c f_{ck}$
N_{pre}	Axial preload
N_u^k	UL of CFST column subject to various loading conditions: $k = A, B, C$ or D
r	Preloading reduction factor, see Eq. (12)
t	Wall thickness of the steel tube

CC